

ABOUT THE USE OF REFLECTANCE TERMINOLOGY IN IMAGING SPECTROSCOPY

*Gabriela Schaepman-Strub¹, Michael Schaepman², Stefan Dangel³,
Thomas Painter⁴ and John Martonchik⁵*

1. Wageningen University, Nature Conservation and Plant Ecology, Wageningen, The Netherlands; gabriela.schaepman@wur.nl
2. Wageningen University, Centre for Geo-Information, Wageningen, The Netherlands; michael.schaepman@wur.nl
3. University of Zurich, Remote Sensing Laboratories, Zurich, Switzerland; dangel@geo.unizh.ch
4. University of Colorado, National Snow and Ice Data Centre, Boulder, USA; tpainter@nsidc.org
5. NASA, Jet Propulsion Laboratory, Pasadena, USA; john.v.martonchik@jpl.nasa.gov

ABSTRACT

Analysing databases, field and airborne spectrometer data, modelling studies and publications, a lack of consistency in the use of definitions and terminology of reflectance quantities can be observed. One example is the term 'BRDF' (bidirectional reflectance distribution function) assigned to significantly differing quantities, ranging from the bidirectional reflectance distribution function to hemispherical-conical reflectance factors. Our contribution summarizes basic reflectance nomenclature articles. Secondly differences of reflectance products are quantified, with special emphasis on wavelength specific effects, to stress the importance of adequate usage of reflectance definitions and quantities. Results from the comparison of directional-hemispherical reflectance versus bihemispherical reflectance and bidirectional reflectance factors versus hemispherical-directional reflectance factors are shown. Differences of these quantities are exemplified using modelling results of a black spruce forest canopy, snow cover, as well as an artificial target. The actual differences in the reflectance products of a remotely sensed surface depend on the atmospheric conditions, the surroundings, topography, and the scattering properties of the surface itself. As these effects are highly wavelength-dependent, the imaging spectroscopy community has to become more specific on the application and definition of reflectance quantities. As of today most delivered reflectance products from imaging spectrometers include the hemispherical illumination component. Thus, product algorithms based on surface reflectance data have to include the actual atmospheric conditions even for nadir view angles, e.g., in the form of a wavelength-specific indication of the ratio of diffuse to direct illumination. The results urge the community to treat reflectance quantities with outmost care and consistency to reduce uncertainties of derived products.

Keywords: Reflectance terminology, BRDF, reflectance, imaging spectroscopy, snow, vegetation.

INTRODUCTION

Imaging spectrometer data and products are constantly improved in quality. Optimization is usually performed at radiance level (enhanced calibration concepts, vicarious calibration, etc.) with uncertainties approaching 4% (1), at reflectance level (atmospheric correction) with uncertainties approaching 5% (2), at product level (sophisticated integration of various sources, assimilation, etc.) with uncertainties approaching 10% (3), but rarely on terminology, where uncertainties can still be much higher than 10%.

The imaging spectroscopy community is developing an increased appreciation of the effects that are induced by the solar illumination and sensor viewing geometry on field, airborne and satellite data. The reflectance anisotropy of the Earth's surfaces and the atmosphere contains unique information about their structure and the optical properties of the scattering elements. The underlying

concept for the characterization of the anisotropy is the bidirectional reflectance distribution function (*BRDF*). It describes the radiance reflected by a surface as a function of a parallel beam of incident light from a single direction into another direction of the hemisphere.

Under natural conditions, i.e. for all ground-based, airborne and spaceborne sensor measurements, the assumption of a single direction of the incident beam does not hold true. Natural light is composed of a direct part, as well as a diffuse component scattered by the atmosphere, and the surroundings of the observed target. The amount and spectral character of the diffuse light irradiating the observed surface thus depend on the atmospheric conditions, as well as on the topography and the scattering properties of the surroundings. Without correction of this diffuse component, observed reflectance quantities depend on actual atmospheric conditions, especially in the Rayleigh scattering dominated wavelength region (400-800 nm), and are not limited to the desired intrinsic directional characteristics of the observed surface. Further, the (instantaneous) field of view (I)FOV of the instrument most often integrates over a large viewing angle and does not allow a single beam observation. Thus, imaging spectrometer measurements do not follow the protocol of directional reflectance quantities and resulting products can only be considered as rough approximations of the surface bidirectional reflectance, a fact that is often neglected.

A physically based terminology, defining various reflectance quantities using the direction of illumination and observation, as well as their opening angle, was proposed by Nicodemus (4), and updated by Martonchik (5). Further, recent advances originating from the Multi-angle Imaging SpectroRadiometer (MISR) science team have led to a more uniform reflectance terminology. The operational MISR data products including different reflectance quantities are a major progress, and give users the opportunity to apply appropriate physical quantities for their investigations.

Despite above-mentioned advancements, physical conditions of measurements and corresponding terminology of at-surface reflectance quantities are still very often neglected by the user community. The loose usage of the term '*BRDF*' is one of the most striking examples. The community performing ground-based multiangular at-surface reflectance measurements often calls acquired quantities *BRDF* or *BRF* (bidirectional reflectance factor) data (e.g., (6)). But the derivation of the *BRDF* from measurements performed under ambient sky (i.e., hemispherical) illumination results in a considerable shape distortion of the resulting function with respect to the true *BRDF* in the visible and near-infrared when no correction for the diffuse part of the illumination is performed, even under clear sky conditions (7). Thus the derived so-called *BRDF* databases do not only reflect intrinsic bidirectional reflectance properties of the observed surface, but also wavelength-dependent effects caused by the diffuse illumination component. This is especially true for diurnal multiangular observations with changing atmospheric conditions throughout the day. Consequently, Martonchik (8) and Lyapustin (7) have developed methods for an accurate atmospheric correction of measured hemispherical-directional reflectance data to enhance the experimental research of anisotropic surface reflectance.

Given the confusion with and neglect of reflectance terminology as exemplified above, the aim of this paper is to summarize the basic nomenclature articles of Nicodemus (4) and Martonchik (5) and make the updated definitions available to the imaging spectroscopy community. This overview helps to identify the correct definition for measured reflectance quantities and processed products, and to apply the appropriate quantity in physical as well as empirical approaches.

The adequate use of reflectance data does not only require a precise, widely distributed and easy to use reflectance terminology, but also an in-depth understanding of spectrodirectional effects. Therefore, the second part of the paper is aiming to demonstrate the importance of adequate use of reflectance definitions and quantities. Uncertainties, introduced by neglecting the physical basis and the corresponding terminology, are exemplified through case studies, with special emphasis on the spectral and directional domain.

This paper systematically highlights differences in at-surface reflectance quantities by their definition. Its focus lies on the geometry of the opening angle of the illumination, i.e., directional and hemispherical extent. A modelling exercise for forest, snow and a highly anisotropic artificial target is performed. Using a variation of the direct to diffuse irradiance ratio in the corresponding models

(i.e. Rahman-Pinty-Verstraete (RPV), discrete-ordinates radiative transfer model (DISORT)), quantitative results of the wavelength-dependent influence of the diffuse component on the hemispherical-directional surface reflectance, i.e., for an illumination of hemispherical extent, are obtained. These results are compared to the quantities obtained for a directional illumination only.

DEFINITIONS

Radiance, reflectance, reflectance factors

Spectral radiance is the most important quantity to be measured in imaging spectroscopy and is the prerequisite for the quantitative analysis of airborne and satellite measurements in the optical domain. It is the radiant flux in a beam per unit wavelength and per unit area and solid angle of that beam. It is usually expressed in the SI units, $W\ m^{-2}\ sr^{-1}\ nm^{-1}$.

Dividing the surface-leaving radiance by the incident radiation onto the surface results in the so-called reflectance. Following the concept of energy conservation, the values of the reflectance are in the inclusive interval 0 to 1. The reflectance factor is the ratio of the radiant flux reflected by a surface to that reflected into the same reflected-beam geometry by an ideal (lossless) and diffuse (Lambertian) standard surface, irradiated under the same conditions. For measurement purposes, a Spectralon panel commonly approximates the ideal diffuse standard surface. Reflectance factors may reach values beyond 1, especially for highly specular reflecting surfaces.

Table 1: Notations used for the definition of at-surface reflectance quantities.

Symbol	Explanation
ρ	reflectance [dimensionless]
R	reflectance factor [dimensionless]
θ	zenith angle, in a spherical coordinate system [rad]
ϕ	azimuth angle, in a spherical coordinate system [rad]
ω	solid angle $\equiv \int d\omega \equiv \iint \sin\theta \cdot d\theta \cdot d\phi$ [sr]
λ	wavelength of the radiation [nm]
f()	function
sub- and superscripts:	
i	incident
r	reflected

The reflectance factor, adapted to the remote sensing problem and respecting particular directional issues, can generally be defined as follows, using the notations in Table 1:




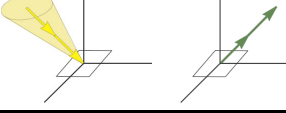
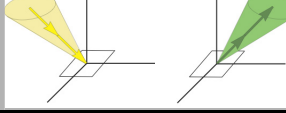

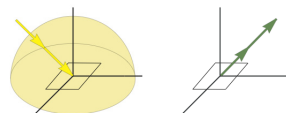

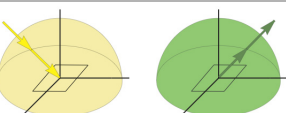
$$R(\theta_i, \phi_i, \omega_i; \theta_r, \phi_r, \omega_r; \lambda),$$

where the direction and the solid angle of the circular cone of the incoming and the reflected radiance are indicated. A refinement of this definition leads to the following special cases:

- ω_i or ω_r are omitted when either is zero (directional quantities).
- If $0 < (\omega_i \text{ or } \omega_r) < 2\pi$, then θ, ϕ describe the direction of the centre axis of the cone (e.g. the line from a sensor to the centre of its ground field of view).
- If $\omega_i = 2\pi$, the angles θ_i, ϕ_i indicate the direction of the incoming direct radiation (e.g., the position of the sun). However, for remote sensing applications, it is often useful to separate the natural incoming radiation into a direct and hemispherical diffuse part. The preferred notation for the geometry of the incoming radiation is then $\theta_i, \phi_i, 2\pi$, thus keeping the position of the sun. It must be noted that in this case, θ_i, ϕ_i do not describe the centre of the cone (2π), except if the sun's position is at nadir.
- If $\omega_r = 2\pi$, θ_r and ϕ_r are omitted.

According to Nicodemus (4), abbreviations for resulting reflectance quantities name the angular characteristics of the incoming radiance first in the term, followed by the angular characteristics of the reflected radiance. This leads to the attributes of spectrodirectional reflectance quantities as illustrated in Table 2.

Table 2: Relation of incoming and reflected radiance terminology used to describe reflectance, with mathematical description of commonly used quantities (see Figure 1 for abbreviations). The labeling with 'Case' corresponds to Nicodemus (4). Grey fields correspond to measurable quantities, whereas the others denote conceptual quantities.

Incoming/ Reflected	Directional	Conical	Hemispherical
<i>Directional</i>	Bidirectional Case 1 $BRDF = f_r(\theta_i, \phi_i; \theta_r, \phi_r; \lambda) [sr^{-1}]$ $BRF = R(\theta_i, \phi_i; \theta_r, \phi_r; \lambda)$ 	Directional-conical Case 2 	Directional-hemispherical Case 3 $DHR = \rho(\theta_i, \phi_i; 2\pi; \lambda)$ 
<i>Conical</i>	Conical-directional Case 4 	Biconical Case 5 	Conical-hemispherical Case 6 
<i>Hemispherical</i>	Hemispherical-directional Case 7 $HDRF = R(\theta_i, \phi_i, 2\pi; \theta_r, \phi_r; \lambda)$ 	Hemispherical-conical Case 8 	Bihemispherical Case 9 $BHR = \rho(\theta_i, \phi_i, 2\pi; 2\pi; \lambda)$ 

Conceptual and measurable reflectance quantities

From a physical point of view, there is the possibility to define special cases, namely conceptual and measurable reflectance quantities. Conceptual quantities of reflectance include the assumption that the size/distance ratio of the illuminating source (usually the sun or lamp) and the observing sensor is zero. They are usually labeled *directional* in the general terminology. Since infinitesimal elements of solid angle do not include measurable amounts of radiant flux, and unlimited small light sources and sensor FOVs do not exist, all measurable quantities of reflectance are performed in the *conical* or *hemispherical* domain of geometrical considerations. Thus, actual measurements always involve non-zero intervals of direction and the underlying basic quantity for all radiance and reflectance measurements is the conical case. The integration of the reflected radiance over a solid angle corresponds e.g. to the opening angle of the sensor. Under field conditions, the incident radiance cone is of hemispherical extent ($\omega = 2\pi sr$). The irradiance can then be divided into a direct sunlight component and a second irradiance component, which is scattered by the atmosphere, the terrain, and surrounding objects, resulting in an anisotropic, diffuse sky illumination. Being a function of wavelength, the ratio of diffuse/direct irradiance highly influences the spectral dependence of directional effects as shown in the quantitative case studies.

Referring to Table 2, the most common measurement setup of satellites, airborne and field instruments corresponds to the hemispherical-conical configuration (Case 8) (e.g., MERIS, ASD Field-

Spec). Albedometers approximate the bihemispherical configuration (Case 9) (e.g., 9). Finally, a typical laboratory setup corresponds to the biconical configuration (Case 5), where a collimated light source illuminates a target that is measured using a non-imaging spectroradiometer (e.g., EGO (10), and LAGOS (11)). The non-zero interval of the sensor’s instantaneous field of view may be neglected for small opening angles and resulting quantities are then reported as bidirectional (laboratory measurements) or hemispherical-directional (small IFOV ground-based, airborne, and spaceborne measurements).

Processing of reflectance quantities

Figure 1 shows the derivation of different reflectance products from satellite data, as implemented in the MISR processing scheme (12). The integration of the at-surface hemispherical-directional reflectance factor (*HDRF* - Case 7) over the viewing hemisphere results in the bihemispherical reflectance (*BHR* - Case 9). Using a modelling approach (e.g., (7,8,9)), the *HDRF* data (Case 7) are further used to derive the bidirectional reflectance factor (*BRF* - Case 1), and finally, directional-hemispherical reflectance (*DHR* - Case 3) can be derived from *BRF* (Case 1) by hemispherical integration over the viewing hemisphere.

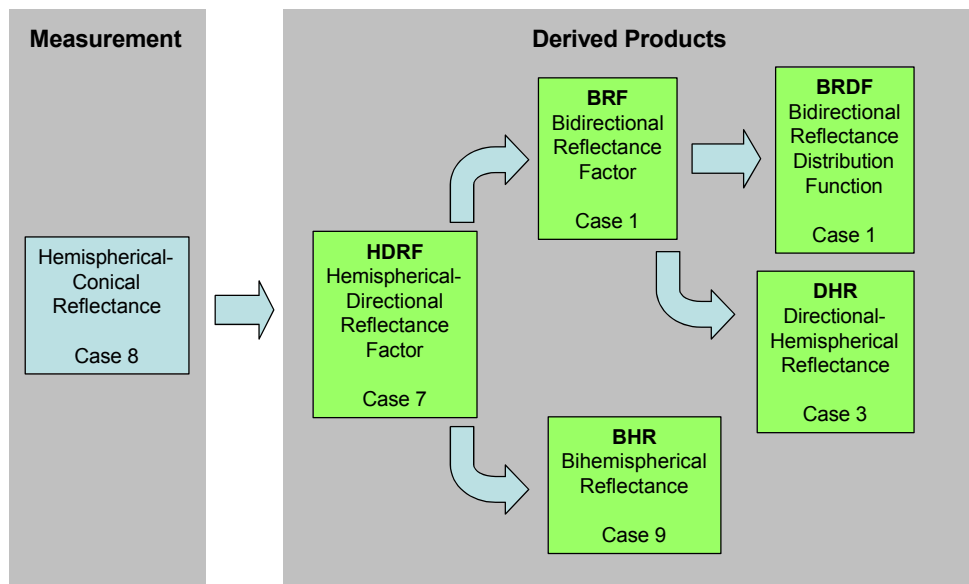


Figure 1: Conceptual data processing chain of airborne and satellite measurements to convert a reflectance measurement (Case 8) into BHR, BRDF, and DHR, as implemented in the MISR processing scheme.

The multiangular measurement configuration of MISR allows for the presented derivation of different reflectance products, using consistent terminology. For many other satellite and airborne systems, the user community is faced with products simply called ‘surface reflectance’, a term not allowing the assignment of the corresponding illumination conditions (i.e., directional or hemispherical) without further knowledge on the preprocessing and corresponding beam geometries. As a consequence, these data are subject to misinterpretation, and subsequently their uncertainties increase.

In imaging spectroscopy, the analysis mostly relies on field or airborne data, which are most often in an experimental stage. As the processing chain differs from sensor to sensor, and algorithm theoretical basis documents (ATBD) are rather short, the processed quantities have to be analysed to determine their exact physical meaning. For the processing chain based on ATCOR (13) used for imaging spectrometer data such as DAIS 7915 and HYMAP sensors at the German Aerospace Centre, the resulting reflectance product most closely can be described as hemispherical-directional reflectance factor (*HDRF*) data (Richter & Martonchik, 2001, personal communication).

CASE STUDIES ILLUSTRATING DIFFERENCES OF REFLECTANCE QUANTITIES

The following case studies highlight differences of the described reflectance quantities using model simulations for a) a vegetation canopy, b) snow cover, and c) an artificial target. The differences of hemispherical versus directional reflectance and reflectance factors (i.e., *BHR* (Case 9) versus *DHR* (Case 3) and *HDRF* (Case 7) versus *BRF* (Case 1)) are computed for the visible to shortwave infrared wavelength range, and different ratios of direct to diffuse illumination conditions.

a) Vegetation canopy reflectance simulations using the RPV model

In the framework of the Boreal Ecosystem-Atmosphere Study (BOREAS), black spruce forest *HDRF* data were observed at eight solar zenith angles (35.1°, 40.2°, 45.2°, 50.2°, 55.0°, 59.5°, 65.0°, 70.0°), using the Portable Apparatus for Rapid Acquisition of Bi-directional Observations of the Land and Atmosphere (PARABOLA) (14). PARABOLA is a two-axis scanning head, three-channel (red, near-infrared, shortwave infrared) radiometer that permits acquisition of radiance data for almost the complete sky- and ground-looking hemispheres. After applying a simple *HDRF* to *BRF* atmospheric correction (15), data of the red spectral band (650-670 nm) were fitted to the parametric Rahman-Pinty-Verstraete (RPV) model (16). This model estimates the bidirectional reflectance of an arbitrary surface as a function of the geometry of illumination and observation. It is a semiempirical nonlinear, three-parameter model, based on the following terms: the overall reflectance level, a parameter representative of the shape of the surface anisotropy (bowl- or bell-shaped), and a description of the predominant scattering direction (forward or backward).

Fitting atmospherically corrected *BRF* data to the RPV resulted in model parameters which were then used in this study to simulate different reflectance quantities of a black spruce canopy under various illumination conditions. The model was run for a solar zenith angle of 30° and increments of direct (*d*) and diffuse irradiance of $d=1.0, 0.8, 0.6, 0.4, 0.2, 0.0$. These irradiance scenarios correspond to *BRF* for $d=1.0$, and *HDRF* for the rest.

As expected for a vegetation canopy, backscattering is the dominating reflectance feature for the black spruce *BRF* data, with a pronounced hot spot at a view zenith of 30° (Figures 2, 3). Adding an isotropic diffuse irradiance component results in *HDRF* data. With decreasing direct irradiance, the anisotropy is smoothed. Finally, the hot spot disappears for a scenario based on diffuse irradiance only. Concentrating on nadir view data, the relative difference between the bidirectional and the hemispherical-directional reflectance factor can be significant, especially for illumination zenith angles around solar noon, approaching the hot spot configuration (Figure 3). Even though absolute differences between single *BRF* and *HDRF* data are numerically small for the selected wavelength range and certain geometries, it becomes obvious that *BRDF* functions can strongly be distorted, when derived from model fits based on *HDRF* instead of *BRF* data.

b) Snow reflectance simulations

This case study presents results from snow directional reflectance simulations, coupling single-scattering parameters and the Discrete-Ordinates Radiative Transfer model (DISORT) (17). DISORT is appropriate for modelling multiple scattering in particulate media and calculates the angular distribution of reflected radiation. The single-scattering parameters used in the model were the single-scattering albedo, extinction efficiency, and the single-scattering phase function, determined with a ray-tracing approach for spheroidal particles (18). Simulation results correspond to a spheroid of minimum and maximum radii of 208 μm and 520 μm , respectively. 20 Legendre moments of the single-scattering phase function were then determined for input to the multiple scattering model. The multiple scattering model was run for a solar zenith angle of 30° and increments of direct (*d*) and diffuse irradiance of $d=1.0, 0.8, 0.6, 0.4, 0.2, \text{ and } 0.0$.

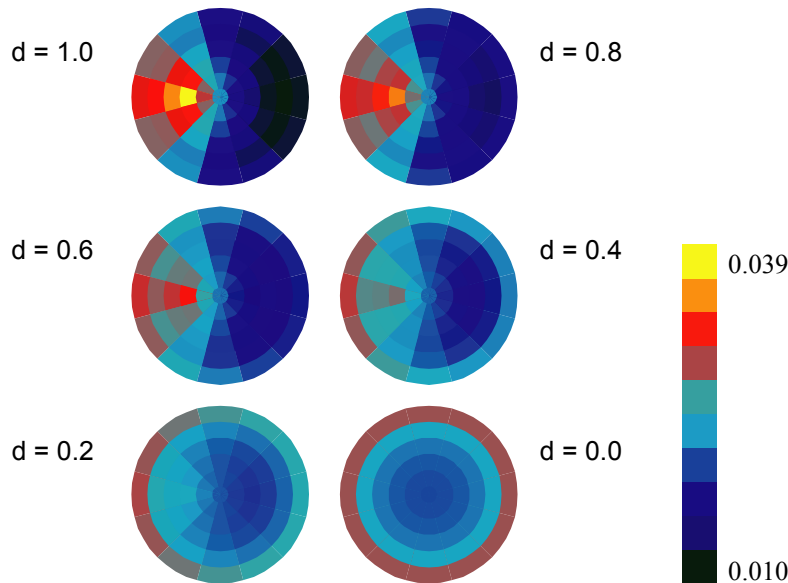


Figure 2: Reflectance factors of a black spruce forest canopy at 650-670 nm as a function of view angle. The direct illumination, at 30° zenith, is from the left. The six plots illustrate the influence of the relative amount of direct illumination (d =direct/diffuse illumination fraction). The top left plot corresponds to pure direct irradiation, thus to BRF data, all others to HDRF data (from $d=0.8$ to $d=0$). The bottom right image corresponds to totally diffuse irradiation ($d=0$).

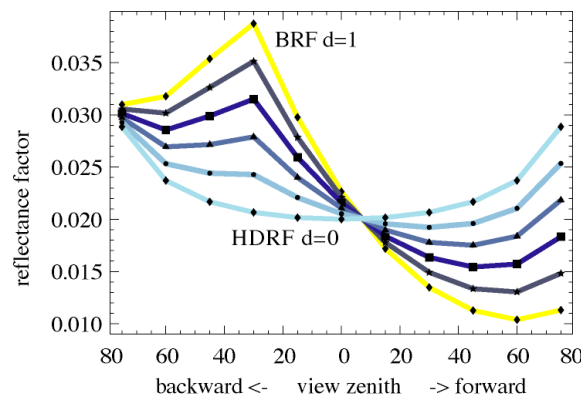


Figure 3: Simulated BRF (d =direct/diffuse illumination fraction =1.0) data for a black spruce canopy in the solar principal plane, and corresponding HDRF for varying direct to diffuse irradiance conditions ($d=0.8$ to $d=0.0$).

In Figure 4, the angular distributions of the irradiance scenarios for wavelength 0.55 μm are shown. The models for $d=1.0$ through $d=0.2$ exhibit a forward reflectance distribution that decreases in magnitude with increasing diffuse component. For the totally diffuse irradiance scenario, the distribution shows a shallow bowl shape. This minimum at nadir results from the angular intersection of the strong forward scattering phase function with the surface. Off-zenith irradiance has a greater chance than zenith irradiance of surviving multiple scatterings due to the orders of magnitude greater single scattering in the forward direction. In other words, zenith irradiance requires far more scattering events to produce reflected radiance than off-zenith. Therefore, the distribution shows greater reflectance at larger view zenith angles. The solar principal plane for these scenarios is given in Figure 5 (top). The bowl-shaped distribution in the principle plane for diffuse irradiance becomes relatively deeper at longer wavelengths (Figure 5 (bottom)), such as 1.03 μm . The 1.03 μm model is shown because this is the wavelength range in which snow reflectance is most sensitive to grain size (19). The enhancement of the bowl shape at greater diffuse irradiance is explained as above coupled with a decrease in the single-scattering albedo at the longer wavelengths. Only for the BRF and $d=0.8$ irradiance cases is the distribution properly forward reflecting.

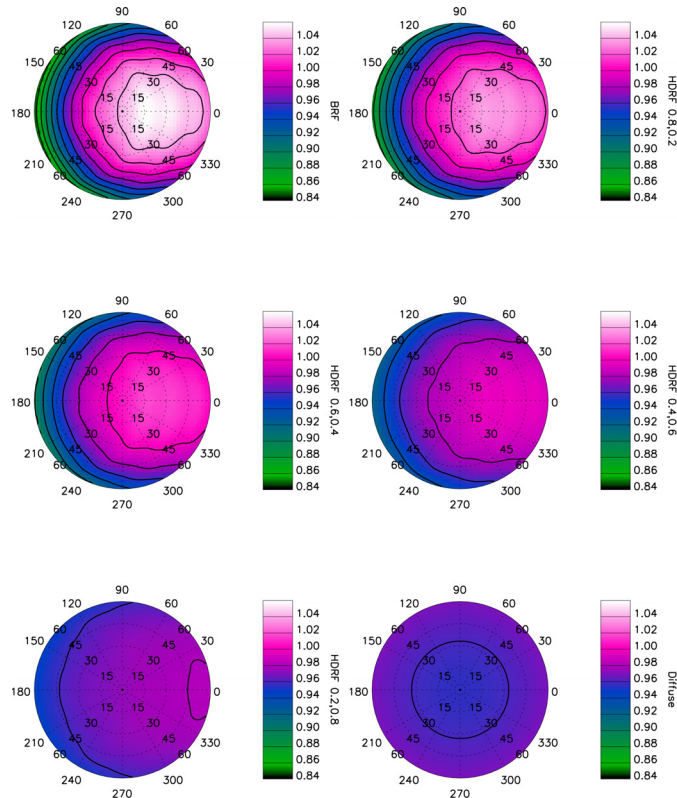


Figure 4: Angular distributions of reflectance for a range of irradiance cases at $0.55 \mu\text{m}$ and solar zenith angle 30° . The six plots illustrate the influence of the relative amount of direct illumination (d = direct/diffuse illumination fraction). The top left plot corresponds to pure direct irradiation, thus to BRF data, all others to HDRF data (from $d=0.8$ to $d=0$). The bottom right plot corresponds to totally diffuse irradiation ($d=0$). The target centre represents the nadir view geometry $(\theta_r, \phi_r) = (0^\circ, 0^\circ)$, radial distance from centre represents the view zenith angle, and the angle about the centre represents the view azimuth angle. The forward reflectance direction is $\phi_r=0^\circ$.

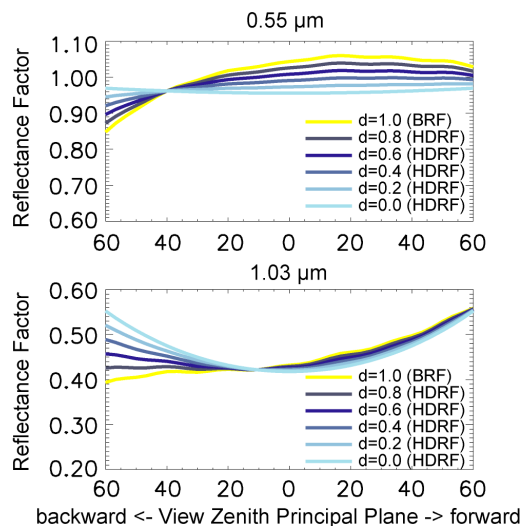


Figure 5: Directional reflectance in the principal plane for a range of irradiance scenarios at wavelengths $0.55 \mu\text{m}$ (top) and $1.03 \mu\text{m}$ (bottom). The plots illustrate the influence of the relative amount of direct illumination (d = direct/diffuse illumination fraction).

c) Artificial target simulations

The third case study concentrates on the reflectance properties of an artificial, highly anisotropic target, which was initially used for a comparison of laboratory goniometric measurements with a radiative transfer model (20). The target consists of a matrix of cubes, carved out of a plate of dur-

aluminum and sanded to avoid specular reflection (Figure 6). The sides of the cubes are 3.3 mm long, the distance between single cubes is 2 mm. The target can be seen as a simple model of a city with blocks and streets.

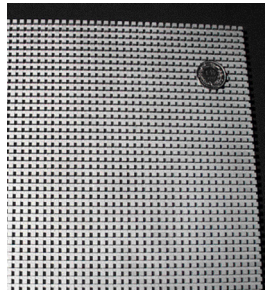


Figure 6: The artificial panel with sanded aluminum surface.

For the following calculations, we used a simple BRDF model of this artificial target, based on geometrical optics. For given view and illumination directions, the model calculates the sum of observed areas that are not shaded. Only single scattering is considered. The surface itself was modeled using the parametric Modified Rahman-Pinty-Verstraete (MRPV) model (16) and the model parameters were fitted to target measurements performed by the Laboratory Goniometer System (LAGOS) (11). The wavelength for all calculations was set to 496 nm. While rotational symmetry is often assumed for natural targets, the aluminum target provides an example for asymmetry.

Figure 7 shows reflectance factors of the artificial target for a variety of direct to diffuse ratios, assuming an incident direct illumination parallel to the 'streets' and an isotropic diffuse radiation. Unlike vegetation, this target is mostly forward scattering. Also the white-sky HDRF is rotational asymmetric due to the rotational asymmetry of the BRF. The target appears brighter when viewed parallel to the 'streets' since, compared to off-parallel viewing, a large part of the 'streets' remains visible even for large view zenith angles.

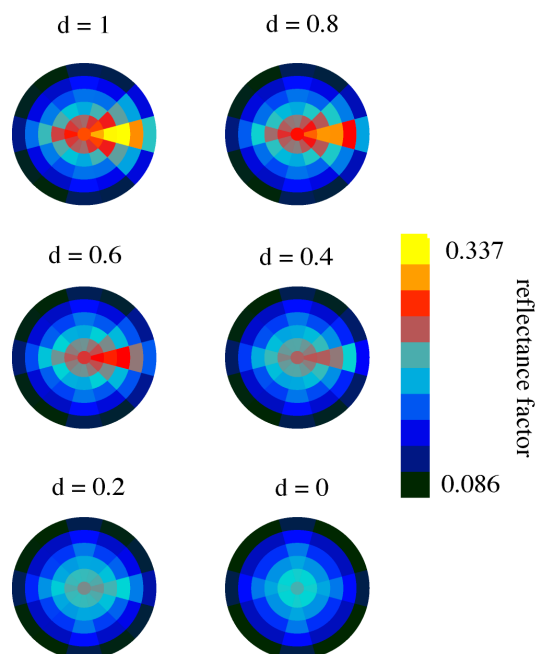


Figure 7: Reflectance factors of the artificial target as a function of view angle. The direct illumination, at 30° zenith, is from the left and parallel to the rows of cubes. The six plots illustrate the influence of the relative amount of direct illumination (between 1 and 0). The top left plot corresponds to direct illumination only ($d=1$), thus to BRF data, whereas all remaining plots display HDRF data (from $d=0.8$ to $d=0$). The bottom right plot corresponds to the white-sky HDRF ($d=0$).

The same data, reduced to the principal plane, are shown in Figure 8. The strong forward scattering, clearly visible in the *BRF*, disappears for lower values of d .

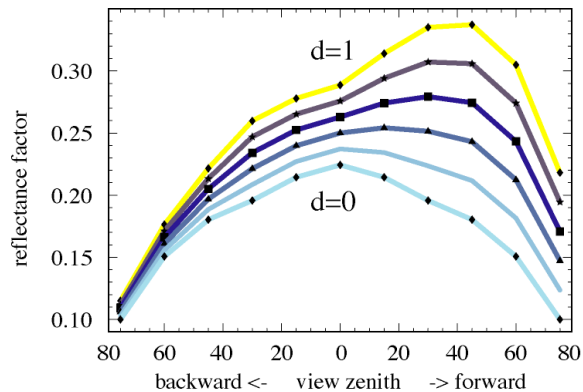


Figure 8: Simulated BRF ($d=1.0$) data for the artificial panel in the solar principal plane, and corresponding HDRF for varying direct to diffuse irradiance conditions ($d=0.8$ to $d=0.0$).

CONCLUSIONS

All remote sensing data depend on the illumination and view geometry of the sensor, as well as on their opening angle. Different reflectance quantities have been defined to describe the corresponding conditions of the measurements. The basis for the proper use of these reflectance quantities is a standardized nomenclature, well known throughout the remote sensing community. This study summarized the nomenclature articles of Nicodemus (4) and Martonchik (5) to give an easy access to the concept. Further, the importance of using the adequate reflectance product is shown. All reflectance measurements performed under natural conditions include a diffuse fraction, which is a function of the atmospheric conditions, the topography, the surroundings of the observed surface, and the wavelength. It thus introduces spectral effects into spectrometer data. The presented case studies are concentrating on the opening angle of the illumination. The effect of varying direct to diffuse irradiance ratio is significant in modelled data. This study is especially addressing the imaging spectroscopy community, due to the wavelength dependence of the shown effects. It shows the importance of including the corresponding illumination and view geometry, and the opening angle in definitions and analysis. Thus, any analysis of uncorrected spectrometer data has to account for wavelength-dependent effects introduced by the diffuse irradiance, which are not intrinsic spectral signatures of the observed scene. In modelling exercises, the diffuse irradiance has to be considered, and eventually be accounted for by indicating the direct/diffuse irradiance fraction wavelength dependently. This study highlights that the presented nomenclature is not only important for multiangular data sets, but also for the characterisation of the irradiance of any remotely sensed reflectance data. Therefore, the publication shall motivate the imaging spectroscopy community to take reflectance nomenclature into account and use the presented common basis for clarity and comparability of data and results.

ACKNOWLEDGEMENTS

This work was supported by the Swiss National Science Foundation, under contract 200020-101517 and through an SNF fellowship grant for prospective researchers. The authors would like to thank Brian Hosgood of the EC Joint Research Centre, Ispra, Italy, for lending the artificial panel for measurements using the FIGOS and LAGOS goniometric facilities.

REFERENCES

- 1 Fox N, J Aiken, J J Barnett, X Briottet, R Carvell, C Frohlich, S B Groom, O Hagolle, J D Haigh, H H Kieffer, J Lean, D B Pollock, T Quinn, M C W Sandford, M Schaepman, K P Shine, W K Schmutz, P M Teillet, K J Thome, M M Verstraete, & E Zalewski, 2003. Traceable radiometry underpinning terrestrial- and helio-studies (TRUTHS). Advances in Space Research, 32: 2253-2261
- 2 Kneubühler M, M E Schaepman, K J Thome, & D R Schläpfer, 2003. MERIS/ENVISAT vicarious calibration over land. In: Sensors, Systems, and Next-Generation Satellites VII, edited by R Meynart, S P Neeck, H Shimoda, J B Lurie & M L Aten (SPIE, Barcelona), 5234, 614-623
- 3 Rast M, F Baret, B van de Hurk, W Knorr, W Mauser, M Menenti, J Miller, J Moreno, M E Schaepman & M Verstraete, 2004. SPECTRA - Surface Processes and Ecosystem Changes Through Response Analysis (ESA Publications Division, Noordwijk), ESA SP-1279(2) 66 pp.
- 4 Nicodemus F, J Richmond, J Hsia, I Ginsberg & T Limperis, 1977. Geometrical Considerations and Nomenclature for Reflectance (NBS, US Department of Commerce, Washington, D.C) 52 pp.
- 5 Martonchik J, C Bruegge & A Strahler, 2000. A review of reflectance nomenclature used in remote sensing. Remote Sensing Reviews, 19: 9-20
- 6 Schonermark M, B Geiger & H P Roeser, 2004. Reflection Properties of Vegetation and Soil (Wissenschaft und Technik Verlag, Berlin) 352 pp.
- 7 Lyapustin A I & J L Privette, 1999. A new method of retrieving surface bidirectional reflectance from ground measurements: Atmospheric sensitivity study. Journal of Geophysical Research-Atmospheres, 104 (D6): 6257-6268
- 8 Martonchik J, 1994. Retrieval of Surface Directional Reflectance Properties Using Ground-Level Multiangle Measurements. Remote Sensing of Environment, 50 (3): 303-316
- 9 Kipp & Zonen, 2000. Instruction Manual CM11 Pyranometer/ CM14 Albedometer (Kipp and Zonen, Delft) 65 pp.
- 10 Koechler, C, B Hosgood, G Andreoli, G Schmuck, J Verdebout, A Pegoraro, J Hill, W Mehl, D Roberts & M Smith, 1994. The European optical goniometric facility: technical description and first experiments on spectral unmixing. In: International Geoscience and Remote Sensing Symposium (IGARSS), Pasadena, 4: 2375-2377
- 11 Dangel, S, M Verstraete, J Schopfer, M Kneubuehler, M Schaepman & K I Itten, 2005. Toward a direct comparison of field and laboratory goniometer measurements. IEEE Transactions on Geoscience and Remote Sensing, 43 (11): 2666-2675
- 12 Martonchik J V, D J Diner, B Pinty, M M Verstraete, R B Myneni, Y Knyazikhin & H R Gordon, 1998. Determination of land and ocean reflective, radiative, and biophysical properties using multiangle imaging. IEEE Transactions on Geoscience and Remote Sensing, 36 (4): 1266-1281
- 13 Richter, R & D Schlapfer, 2002. Geo-atmospheric processing of airborne imaging spectrometry data. Part 2: atmospheric/topographic correction. International Journal of Remote Sensing, 23 (13): 2631-2649
- 14 Deering D W, T F Eck & B Banerjee, 1999. Characterization of the Reflectance Anisotropy of Three Boreal Forest Canopies in Spring-Summer. Remote Sensing of Environment, 67: 205-229

- 15 Tanre D, M Herman & P Y Deschamps, 1983. Influence of the Atmosphere on Space Measurements of Directional Properties. Applied Optics, 22 (5): 733-741
- 16 Engelsen O, B Pinty, M Verstraete & J V Martonchik, 1996. Parametric bidirectional reflectance factor models: evaluation, improvements and applications (EC Joint Research Centre, Ispra, Italy) 114 pp.
- 17 Stamnes K, S C Tsay, W Wiscombe & K Jayaweera, 1988. Numerically Stable Algorithm for Discrete-Ordinate-Method Radiative-Transfer in Multiple-Scattering and Emitting Layered Media. Applied Optics, 27 (12): 2502-2509
- 18 Macke A & M I Mishchenko, 1996. Applicability of regular particle shapes in light scattering calculations for atmospheric ice particles. Applied Optics, 35 (21): 4291-4296
- 19 Nolin A W & J Dozier, 2000. A hyperspectral method for remotely sensing the grain size of snow. Remote Sensing of Environment, 74 (2): 207-216
- 20 Govaerts Y, M Verstraete & B Hosgood, 1997. Evaluation of a 3-D Radiative Transfer Model Against Goniometer Measurements on an Artificial Target. International Journal of Remote Sensing, 1: 131-136